Proceedings of ASME Turbo Expo 2011
GT2011
June 6-10, 2011, Vancouver, British Columbia, Canada

GT2011-45345

IMPROVED MAP SCALING METHODS FOR SMALL TURBOCHARGER COMPRESSORS

Benedikt Ernst, Jasper Kammeyer, and Joerg R. Seume
Institute of Turbomachinery and Fluid Dynamics
Department of Mechanical Engineering
Leibniz Universitaet Hannover
Appelstrasse 9, 30167 Hannover, Germany
E-mail: Ernst@tfd.uni-hannover.de

ABSTRACT
Today engine performance simulations are essential in the preliminary design of turbocharged combustion engines, e.g. when matching the engine and the turbocharger. In order to optimize this matching process and to enable a preliminary selection of different turbocharger types and sizes, realistic modifications of the compressor and turbine maps are needed.
This paper discusses several published approaches for compressor diameter scaling methods. In this context, an improved method to determine the efficiency changes due to diameter scaling of small turbocharger compressors is presented. Besides diameter scaling, trim scaling is a possibility to change the operating range of a compressor. Therefore, a trim scaling method is provided. In order to validate the scaling methods, scaled compressor maps are compared to measured nominal maps.

NOMENCLATURE

A	Area
a	Slope
b_2	Impeller blade outlet width
c	Velocity
D	Diameter
EF	Efficiency-factor
M_{u2}	Circumferential Mach number
$\dot{m}$	Mass flow
N	Rotational speed
p_{1t}	Total inlet pressure
R	Ideal gas constant
Re	Reynolds number
SF	Scaling factor
T	Temperature
U	Circumferential speed
Δh_{is}	Isentropic enthalpy change
η	Efficiency
κ	Isentropic exponent
μ	Dynamic viscosity of the fluid
Π	Similarity variable
π	Total-total pressure ratio
ρ	Density
ϕ	Mass flow coefficient
ψ	Head coefficient

Subscripts

b	Baseline quantity
m	Measured quantity
s	Scaled quantity
t	Total quantity
hub	Hub
red	Reduced quantity
ref	Reference quantity
1	Inlet condition
2	Impeller outlet condition

INTRODUCTION
The scarcity of fossil fuels and the limitations due to emissions and CO_2 legislations require a continuous reduction of fuel consumption and exhaust emissions of combustion engines. Apart from future concepts like fuel cells and electrification of the powertrain, downsized engines are a promising technology to achieve current and future standards. Therefore, an optimal matching of the engine and the turbocharger is essential in order to develop fuel-efficient engines.

In the preliminary design phase engine performance simulations are used to match the engine and the turbocharger.

These simulations require turbocharger maps which are obtained from turbocharger test stands. During the matching process, car and engine manufactures usually possess only a small number of turbocharger maps and limited geometric information.

In order to optimize the matching process and to enable a preliminary selection of the turbocharger concerning type and size, realistic modifications of the compressor and turbine maps are needed. In the turbocharger industry it is a common method to use one impeller blade design for different diameters and trims to cover a wider operating and performance range. Therefore, the objective of this paper is to permit a simple diameter and/or trim scaling method for turbocharger compressors which allow scaling in a range of *±20%*. To enable the scaling method for daily technical use, only a baseline compressor map and very limited geometric information are needed.

There is only a small number of publications dealing with the scaling of turbocharger maps. Generally, the similarity laws provide a simple and effective approach to scale an existing design from one size to another [1]. The principle of similitude and non-dimensional parameters is described in several publications e.g. [1-6]. Two machines are similar if geometric and dynamic similarity is given. Geometric similarity means that the corresponding geometric dimensions of both machines are proportional to one another. In the case of dynamic similarity, the velocity and force vectors are parallel and proportional in the corresponding local points. This results in the assumption that the non-dimensional parameters have to be equal [5]. However in practice it is impossible to satisfy all these requirements simultaneously. Therefore, in most cases the Reynolds number cannot be scaled correctly and a specific correction is necessary [1]. In a limited range, only a small impact of the Reynolds number on the pressure was found by Schleer and Abhari [7] for the scaling of small turbocharger compressors. However, the Reynolds number shows a significant impact on the efficiency, as shown by Pampreen [8], Simon and Buelskaemper [9], Casey [10], and Strub et al. [11]. This paper deals with the use of similarity laws for scaling the maps of small turbocharger compressors. In this context, an empirical approach to determine the efficiency changes due to diameter scaling is presented.

Besides diameter scaling, trim scaling is a possibility to change the operating range of a compressor. An increasing trim will shift the compressor map to higher flow rates and a decreasing trim to lower flow rates. The test data from Rogers [12] shows that trim scaling is an effective method of changing the compressor flow capacity while preserving acceptable efficiencies. In addition Sapiro [13] and Engeda [14] did experimental investigations with various impeller contours. However, as far as the authors know, no physical or empirical correlations of the compressor map parameters with different trims are published. Therefore, in addition to the diameter scaling a trim scaling method with an empirical correction function is presented.

DATABASE AND METHODOLOGY

In order to derive the empirical correlations and correction functions, two commercially used standard turbocharger compressor types are chosen. The impeller outlet diameter of type A compressors varies in a range of *46 mm* to *58 mm* and of type B compressors in a range of *31 mm* to *42 mm*. The trim of type A compressors is *74* and of type B compressors *67*. Each type indicates one standard product series with the same impeller geometry, housing geometry, and the same trim design. However, type A and type B compressors have different geometries, trim designs and also different sizes.

For diameter scaling comparisons there are three maps of type A compressors, and two maps of type B compressors. This results in four diameter upscaling and four diameter downscaling comparisons. All geometric dimensions of the impeller and the housing change with the same ratio as the impeller outlet diameter. The diameter scaling factors for both compressor types are given in Table 1 and Table 2. Furthermore, in Figure 1 the mass flow coefficient and the head coefficient for the design points are shown.

Table 1 Diameter scaling factors for type A compressors

	small size	medium size	large size
small size	1.00	1.11	1.22
medium size	0.90	1.00	1.10
large size	0.82	0.91	1.00

Table 2 Diameter scaling factors for type B compressors

	small size	large size
small size	1.00	1.24
large size	0.80	1.00

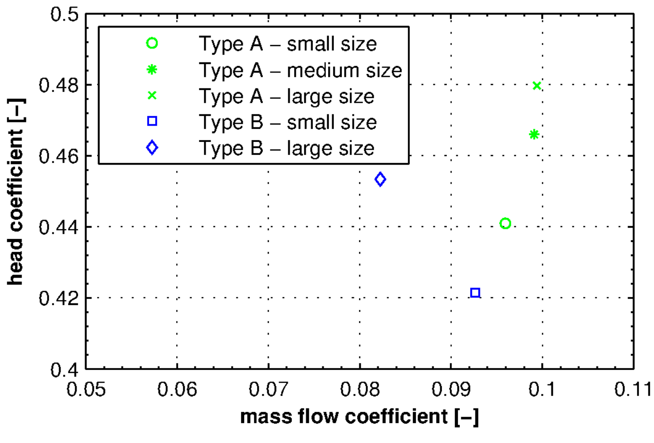

Figure 1 Mass flow coefficient and head coefficient for the design points of the different compressors

In addition to the measured compressor maps with different diameters, there are three type A compressors with different trims and constant impeller outlet diameters. The impeller contour is trimmed in the way that the impeller geometry, the housing geometry, and the trim design remain unchanged.

Since, the outlet diameter is held constant the trim changes with the same ratio as the impeller inlet diameter. The given trim scaling factors for type A compressors are shown in Table 3. Further it should be mentioned that the compressor with the lowest trim is the largest compressor of type A.

Table 3 Trim scaling factors for type A compressors

	low trim	medium trim	high trim
low trim	1.00	1.04	1.08
medium trim	0.96	1.00	1.04
high trim	0.93	0.96	1.00

The given compressor maps were measured on standard turbocharger test stands with typical measurement uncertainties. Because of confidentiality it is not possible to publish further geometric details, and the real measurement data of both compressor types. Therefore, the axis labels in the following diagrams and compressor maps are normalized with freely selected values.

SIMILARITY AND NON-DIMENSIONAL PARAMETERS

The principle of similitude is based on the Buckingham Π-theorem [15] which is a mathematical method to describe similar physical systems. With the Π-theorem it is possible to define several non-dimensional parameters. In agreement with Lakshminarayana [2], Dufour et al. [16] give a set of four non-dimensional Π-products or similarity variables to describe the performance of a centrifugal compressor.

If two compressors are geometrically similar and the similarity variables are equal for both machines, the pressure ratio and the efficiency are also identical. While scaling an existing turbocharger compressor to another size, it is assumed that the gas (air) properties do not change. Dufour et al. [16] show that exact similarity cannot be realized. For this reason, some additional assumptions are necessary.

Besides the above mentioned Π-products, commonly used non-dimensional parameters are the mass flow coefficient ϕ, the head coefficient ψ, the blade tip Mach number M_{u2} and the Reynolds number Re. But there are several different definitions of these parameters. In this paper the following definitions are used (Equations 1 to 4). Dufour et al. [16] have shown that these non-dimensional parameters can be derived from the Π-products or the similarity variables.

$$\phi = \frac{\dot{m}}{\rho_{1t} U_2 D_2^2} = \frac{\dot{m} R T_{1t}}{p_{1t} N D_2^3} \tag{1}$$

$$\psi = \frac{\Delta h_{is}}{U_2^2} = \frac{\frac{\kappa}{\kappa - 1} R T_{1t} \left(\pi^{\frac{\kappa-1}{\kappa}} - 1 \right)}{N^2 D_2^2} \tag{2}$$

$$M_{u2} = \frac{U_2}{\sqrt{\kappa R T_{1t}}} = \frac{N D_2}{\sqrt{\kappa R T_{1t}}} \tag{3}$$

$$\mathrm{Re} = \frac{\rho_{1t} D_2 U_2}{\mu} = \frac{N D_2^2 p_{1t}}{\mu R T_{1t}} \tag{4}$$

DIAMETER SCALING

Due to the fact that exact similarity cannot be realized [16], it is assumed that the Reynolds number is nearly free to vary, if the diameter scaling factors are not too large. Furthermore, it is assumed that the gas properties κ, μ, and R are constant. This is called 'Partial similarity: Re-free scaling' [16] or 'Level 1 design: stage scaling' [1].

For reasons of comparability of different measured turbocharger compressor maps the rotational speed and the mass flow are reduced to a reference condition (p_{ref}, T_{ref}), which is constant for comparable compressors. According to SAE J922 the reduced quantities are defined as:

$$N_{red} = N \sqrt{\frac{T_{ref}}{T_{1t}}} \, , \tag{5}$$

$$\dot{m}_{red} = \dot{m} \frac{\sqrt{T_{1t}/T_{ref}}}{p_{1t}/p_{ref}} \, . \tag{6}$$

For the following scaling comparisons the quantities of the baseline compressor will be denoted with subscript '*b*' and of the scaled compressor with subscript '*s*'. Considering the given assumptions and the reduced quantities (Equations 5 and 6), Equations 1 and 3 result in:

$$\frac{\phi_s}{\phi_b} = 1 = \frac{\dfrac{\dot{m}_s R T_{1t}}{p_{1t} N_s D_{2s}^3}}{\dfrac{\dot{m}_b R T_{1t}}{p_{1t} N_b D_{2b}^3}} = \frac{\dot{m}_{red,s}}{\dot{m}_{red,b}} \frac{N_{red,b}}{N_{red,s}} \frac{D_{2b}^3}{D_{2s}^3} \, , \tag{7}$$

$$\frac{M_{u2,s}}{M_{u2,b}} = 1 = \frac{\dfrac{N_s D_{2s}}{\sqrt{\kappa R T_{1t}}}}{\dfrac{N_b D_{2b}}{\sqrt{\kappa R T_{1t}}}} = \frac{N_{red,s}}{N_{red,b}} \frac{D_{2s}}{D_{2b}} \, . \tag{8}$$

With the diameter scaling factor

$$SF_D = \frac{D_{2s}}{D_{2b}} \, , \tag{9}$$

Equation 8 turns to:

$$\frac{N_{red,s}}{N_{red,b}} = \frac{D_{2b}}{D_{2s}} = \frac{1}{SF_D} . \quad (10)$$

The mass flow relation results from Equations 7, 9 and 10 as:

$$\frac{\dot{m}_{red,s}}{\dot{m}_{red,b}} = \frac{D_{2s}^2}{D_{2b}^2} = SF_D^2 . \quad (11)$$

Schleer and Abhari [7] have shown that a reduction in Reynolds number by a factor of *3.3* results in a drop of *0.5%* in the pressure ratio. In the present paper the changes in Reynolds number are significantly smaller. Therefore, it is assumed that the pressure ratio is nearly constant:

$$\pi_s = \pi_b . \quad (12)$$

Equations 10, and 11 give an overview of commonly known scaling relations. These are for example also given in [1] and [4].

EFFICIENCY ADJUSTMENT

Except for the efficiency, all necessary scaling relations are given (Equations 10, 11 and 12). The loss mechanisms of radial compressors are very complex and the diameter scaling will affect them in different ways. Therefore, an empirical approach is used to consider the effects on the efficiency. As discussed in the previous sections, the Reynolds number changes if the compressor is scaled with the similarity variables. In the literature several approaches are discussed how the Reynolds number effects the efficiency. Wright [17] gives an overview of the older exponential scaling algorithms and the formulations which are based on friction factor correlations, for example of Casey [10] and Strub et al. [11]. He concludes that the simple and non-rigorous exponential method performs nearly as well as the methods which are based on friction factor correlations.

To evaluate the different approaches for small turbocharger compressors, Casey’s formulation is compared with an exponential method called n-scaling method. The n-scaling method is based on the work of Moody (1925, 1944) and Ackeret (1930) [17]. A generic representation has the form below:

$$\frac{1-\eta_s}{1-\eta_b} = \left(\frac{\mathrm{Re}_b}{\mathrm{Re}_s}\right)^n . \quad (13)$$

With the definition of the Reynolds number (Equation 4) and the assumptions that the inlet conditions and the gas properties do not change, the efficiency of the scaled compressor is given as:

$$\eta_s = 1 - \frac{1-\eta_b}{\left(\frac{D_s}{D_b}\right)^n} . \quad (14)$$

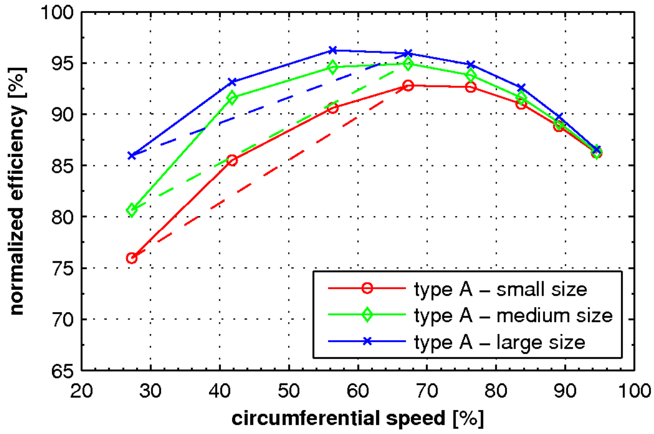

Figure 2 Best-efficiency lines with connecting lines (dashed lines)

The exponent n is an empirical constant. In the literature the values of n are in a range from *0.1* to *0.625* [17]. For the comparison with Casey's method, values of *0.1*, *0.45*, and *0.5* are chosen for n. In order to evaluate the different approaches and to determine the efficiency changes, the measured type A and type B compressor maps with different diameters are used (c.f. Table 1 and Table 2).

Figure 2 shows the measured best-efficiency lines of type A compressors. The best-efficiency line indicates the operating points with the best efficiency on each speed line. It is obvious that an increasing diameter causes an increasing efficiency, especially at low speeds. Figure 3 shows the relative deviations between the scaled and the measured maximum efficiencies for the n-scaling method with different values of n as well as Casey's method. With the scaled efficiency η_s and the comparable measured efficiency η_m, the relative deviation is defined as:

$$\Delta = \frac{\eta_s - \eta_m}{\eta_m} . \quad (15)$$

The type B compressors have the diameter scaling factors 0.8 and 1.24 (c.f. Table 2). All other data points are taken from comparisons of type A compressors. It is shown that the n-scaling method with n=*0.1* has the largest relative deviation. On average, the n-scaling method with n=*0.45* has the smallest relative deviation and it is even better than Casey's method. This is somewhat surprising, because Wright [17] shows a clear advantage of correctly formulated scaling algorithms over empirically based, simple exponential methods. One reason for this discrepancy could be that Casey uses radial compressors with impeller outlet diameters larger than *300 mm* which is considerable larger than typical turbocharger compressors for downsizing applications. To use Casey's method for small turbocharger compressors, some adjustments could be necessary. Due to the smallest relative deviations and the simplicity, the n-scaling method with *n=0.45* is used in the following to determine the scaled maximum efficiency:

$$\eta_{s,\max} = 1 - \frac{1-\eta_{b,\max}}{\left(\frac{D_{2s}}{D_{2b}}\right)^{0.45}} . \qquad (16)$$

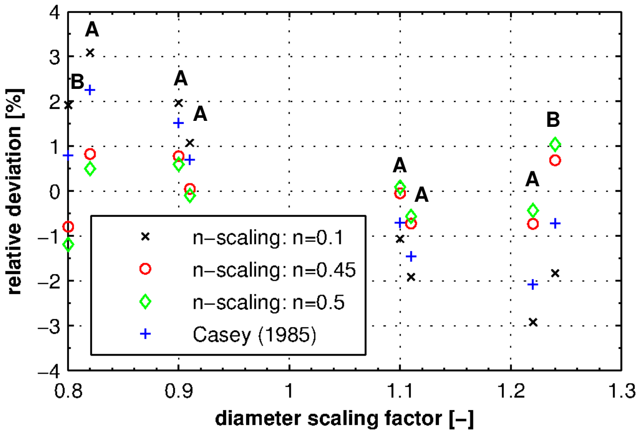

Figure 3 Relative deviations between the scaled and measured maximum efficiencies for different methods (A and B indicate the compressor types)

Further investigations have shown that the n-scaling and/or Casey's method only provides acceptable results at the maximum efficiency regarding the given compressor maps. Therefore, additional empirical correlations will be derived to adjust the best-efficiency line for larger and lower circumferential speeds than the optimum speed. For this reason a simple efficiency-factor *EF* which is a function of the circumferential speed is implemented.

It is noticeable that the best-efficiency lines of the different type A compressors reach nearly the same point at the maximum circumferential speed (c.f. Figure 2). This is also the case for type B compressors. For this reason, the following relation is suggested at the maximum circumferential speed:

$$EF\left(U_{2red,\max}\right) = \frac{\eta_s\left(U_{2red,\max}\right)}{\eta_b\left(U_{2red,\max}\right)} = 1 . \qquad (17)$$

The second reference point results from Equation 16 at the optimal circumferential speed:

$$EF\left(U_{2red,opt}\right) = \frac{\eta_s\left(U_{2red,opt}\right)}{\eta_b\left(U_{2red,opt}\right)} = \frac{\eta_{s,\max}}{\eta_{b,\max}} . \qquad (18)$$

In Figure 2 it is shown that the differences between the best-efficiency lines rise with decreasing circumferential speed. Therefore, the third reference point is at the lowest circumferential speed. This is determined with the help of the slope of the connecting lines from the maximum efficiency to the efficiency with the lowest circumferential speed which are measured to the same circumferential speed (c.f. dashed lines in Figure 2). It is assumed that the maximum efficiencies of the baseline and the scaled compressor are located at the same circumferential speed. For the comparison of the measured efficiencies in Figure 2, the maximum efficiency of the large size compressor is located at a different circumferential speed compared to the small and medium size compressor. However, it is a reasonable assumption because in Figure 2 the efficiency differences of circumferential speed between *56%* and *67%* is lower than the possible error of the maximum efficiency adjustment with Equation 16.

The slope of the connecting lines in Figure 2 decreases with increasing diameter for the same compressor type. Figure 4 shows a nearly linear correlation of the slope ratio and the diameter scaling factor.

With this correlation it is possible to determine the slope of the connecting line of the scaled compressor and hence the efficiency at minimum circumferential speed:

$$a_s = a_b\left(-2.1\frac{D_{2s}}{D_{2b}} + 3.1\right) \qquad \text{for } \frac{D_{2s}}{D_{2b}} \geq 1 , \qquad (19a)$$

$$a_s = \frac{a_b}{-2.1\frac{D_{2b}}{D_{2s}} + 3.1} \qquad \text{for } \frac{D_{2s}}{D_{2b}} < 1 , \qquad (19b)$$

$$\eta_s\left(U_{2red,\min}\right) = \eta_{s,\max} - a_s\left(U_{2red,opt} - U_{2red,\min}\right) . \qquad (20)$$

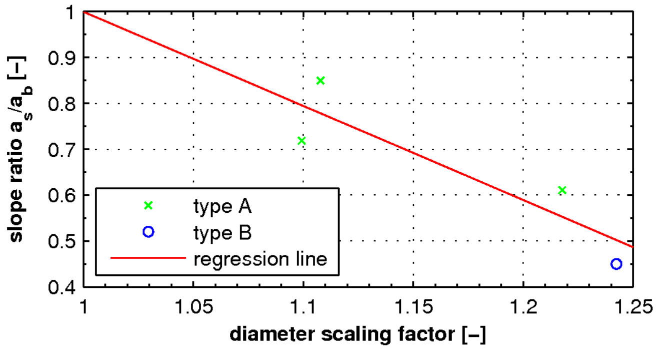

Figure 4 Correlation of the diameter scaling factor and the slope ratio

With Equation 20 and the efficiency of the baseline compressor the third reference point of the efficiency-factor function can be determined:

$$EF\left(U_{2red,\min}\right) = \frac{\eta_s\left(U_{2red,\min}\right)}{\eta_b\left(U_{2red,\min}\right)} . \qquad (21)$$

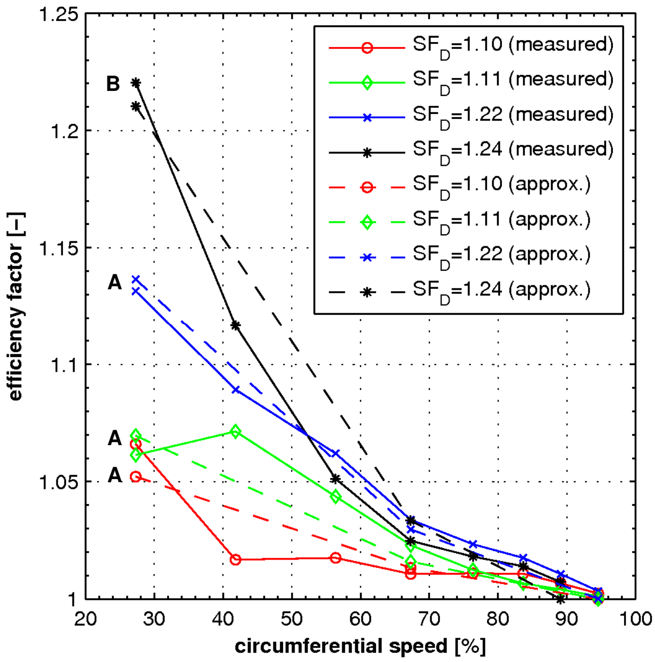

Figure 5 Efficiency-factor depending on the circumferential speed to match the best-efficiency line (A and B indicate the compressor types)

The efficiency-factor correlations for the best-efficiency lines are displayed in Figure 5 as comparison of the measured efficiency factors (solid lines) and the approximated efficiency-factors (dashed lines). The three reference points are also displayed in Figure 5 (dashed lines). In order to minimize the approximation error, the operating range is separated in two regions with a linear dependence between the circumferential speed and the efficiency-factor in each region:

$$U_{2red,\min} \leq U_{2red} < U_{2red,opt} \tag{22a}$$

and

$$U_{2red,opt} \leq U_{2red} \leq U_{2red,\max} \,. \tag{22b}$$

The error between the measured and the approximated efficiency-factor seems to be very serious in Figure 5. However, except of a few points the relative approximation error is lower than ±*2%* and for high circumferential speeds the error is even smaller than ±*1%* (see Figure 6). The comparison of type B compressors corresponds to the data points with the scaling factor 1.24, all other data points are comparisons of type A compressors.

After the efficiency-factor is determined for the complete best-efficiency line, the efficiency of the scaled compressor is given (Equation 23). Thereby it is assumed that the efficiency-factor is constant for a complete speed line of a compressor map.

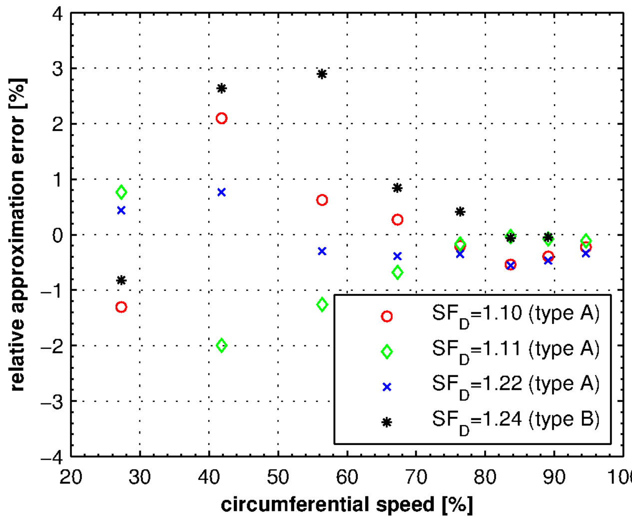

Figure 6 Relative deviations between the scaled and measured best-efficiency lines

$$\eta_s = EF\left(U_{2red}\right) \cdot \eta_b \tag{23}$$

TRIM SCALING

In this paper, the trim of a compressor is defined as the ratio of the inlet and outlet diameter in percent (Equation 24). This is also the case for the given compressor maps.

$$Trim = \frac{D_1}{D_2} \cdot 100 \tag{24}$$

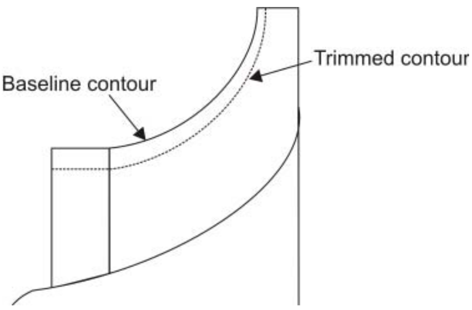

Figure 7 Example of impeller contour trimming

There are several possibilities to vary the trim and therefore the mass flow range. Starting from a baseline impeller the contour will be trimmed in the way that the impeller geometry, the housing geometry, and the trim design remain unchanged. An Example of impeller contour trimming, as considered in the present paper, is shown in Figure 7. Furthermore, the impeller leading edge angle and local curvature do not change. However, the impeller leading edge angle at the casing will be different.

Thereby, the outlet diameter is held constant and the trim changes with the same ratio as the impeller inlet diameter:

$$\frac{Trim_s}{Trim_b} = \frac{D_{1s}}{D_{2b}}. \tag{25}$$

For small trim variations it is assumed that for constant rotational speeds the changes in pressure ratio and efficiency are negligible. Based on measured compressor maps with different trims (c.f. Table 3) it will be seen in the next section that this is a reasonable assumption. Therefore, only a mass flow adjustment is necessary. For the baseline and the scaled compressor the continuity equations at the impeller inlet are formulated and set into relation in order to determine the mass flow changes:

$$\frac{\dot{m}_s}{\dot{m}_b} = \frac{\rho_{1s} \cdot c_{1s} \cdot A_{1s}}{\rho_{1b} \cdot c_{1b} \cdot A_{1b}}, \tag{26}$$

with the impeller inlet area

$$A_1 = \frac{\pi}{4}\left[\left(\frac{Trim}{100} \cdot D_2\right)^2 - D_{1,hub}^2\right]. \tag{27}$$

Ambient conditions are assumed for the total inlet pressure and temperature. Therefore, they are not affected by trim scaling and the mass flow ratio in Equation 26 can be replaced by the ratio of the reduced mass flows. Further investigations have shown that the air density at compressor inlet is nearly constant, so the reduced mass flow changes depend only on the area ratio and the velocity ratio. As a result, the reduced mass flow of the scaled compressor is given as:

$$\dot{m}_{red,s} = \dot{m}_{red,b} \frac{\left[\left(\frac{Trim_s}{100} \cdot D_2\right)^2 - D_{1,hub}^2\right]}{\left[\left(\frac{Trim_b}{100} \cdot D_2\right)^2 - D_{1,hub}^2\right]} \frac{c_{1s}}{c_{1b}}. \tag{28}$$

Initially it was assumed that the velocity ratio is 1, but this results in large deviations between the scaled and the measured map at the choke line. In order to determine the velocity ratio at the choke line, an empirical correlation is derived from the measured maps. In Figure 8 these correlations are shown for three trim variations. It is assumed that the measured ratios can be approximated with a quadratic function. The quadratic function has an extreme value at the minimum circumferential speed and a value of 1 at the maximum circumferential speed. The value at the maximum circumferential speed is constant and independent from the trim scaling factor. Therefore, only a correlation between the trim scaling factor and the inlet velocity ratio is required to estimate the second reference point of the approximation function. This correlation is displayed in Figure 9.

If the inlet velocity ratio is estimated with the quadratic approximation and the correlation of Figure 9, the scaled reduced mass flow can be determined with Equation 28. Again, it is assumed that the inlet velocity ratio is constant on a constant speed line. As mentioned above, all other quantities of the compressor map remain constant.

VALIDATION – COMPARISION OF SCALED AND MEASURED COMPRESSOR MAPS

In order to validate the diameter and trim scaling methods, different scaling examples, each with the baseline, the scaled and the measured compressor maps are plotted. In addition to the compressor maps, the best-efficiency lines are also shown (see Figure 10 to 17). Furthermore, for two scaling examples the efficiency lines with constant rotational speed are displayed in Figure 18 and 19 (Annex A).

It was not possible to carry out a complete error analysis with the existing measured data, since the detailed measurement uncertainties of the different turbocharger test stands are not known. The uncertainty of all measured compressor maps has the same magnitude which are typical for commercial turbocharger test stands. However, to visualize the deviations between the scaled and the measured maps, the error bars in the maps indicate a relative deviation of ±2% of each quantity of the measured nominal maps.

Compared to the measured nominal maps, the relative deviations of the scaled maps are in a range of ±2%. Only the deviations at the surge or choke line are a little bit larger in some cases. This could be the result of geometry changes which differ from the assumptions for the scaling methods.

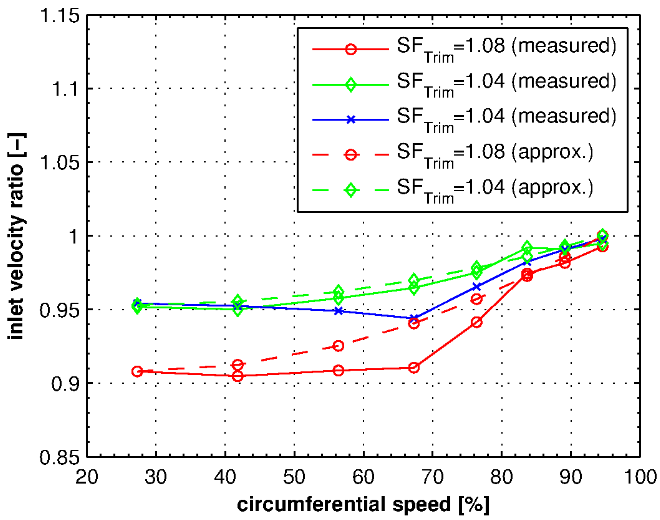

Figure 8 Inlet velocity ratio at the choke line

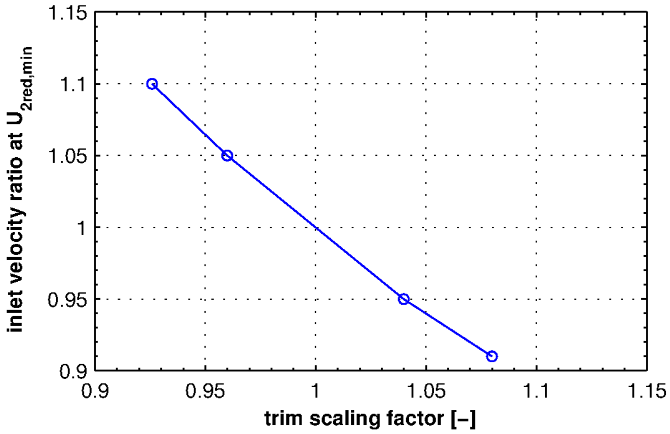

Figure 9 Inlet velocity ratio for different trim scaling factors at $U_{2red,min}$

LIMITATIONS OF THE SCALING RELATIONS

The previous section showed that there is a correlation between increasing scaling ratios and the deviations between the scaled and the measured nominal map. However, they are in an acceptable range. In order to avoid large scaling errors it is recommended to scale the diameter and/or trim only in a range of ±*20%*.

Diameter scaling is based on the assumption of geometric similitude. For trim scaling it is assumed that the impeller outlet diameter and the trim design is held constant, therefore the impeller inlet diameter changes with the same ratio as the trim. These assumptions of geometry changes concerning diameter and trim scaling could possibly differ from common design practices for turbocharger compressors and hence explain some deviations between the scaled and measured maps. Therefore, it is important to consider the limitations of these scaling methods.

CONCLUSIONS

The changes in pressure ratio, mass flow, and rotational speed resulting from diameter modifications are computed based on similarity rules and non-dimensional performance parameters. In order to account for efficiency changes, a simple efficiency-factor function based on an empirical correlation is shown to match the best-efficiency line of the compressor maps. The efficiency-factor is constant for a complete speed line of a compressor map.

The comparison of different measured compressor maps shows that for constant rotational speeds and for small trim variations the changes in pressure ratio and efficiency are negligible. Therefore, for the use of trim scaling methods, only a mass flow adjustment is necessary. The mass flow adjustment presented in this paper is based on the continuity equation and an empirical correction function which accounts for inlet velocity changes.

In order to avoid large scaling errors, it is recommended to scale the diameter and/or trim only in a range of ±*20%*. Using the improved scaling methods, the relative deviations of the scaled maps are in a range of ±*2%*, compared to the measured nominal maps. However, it is recommended to validate the present methods with further compressor maps.

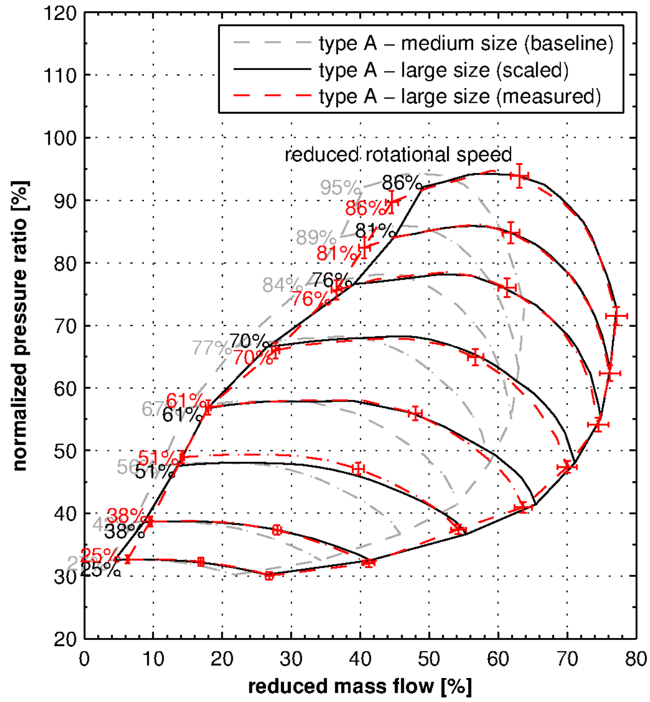

Figure 10 Map comparison with a diameter scaling factor of 1.1

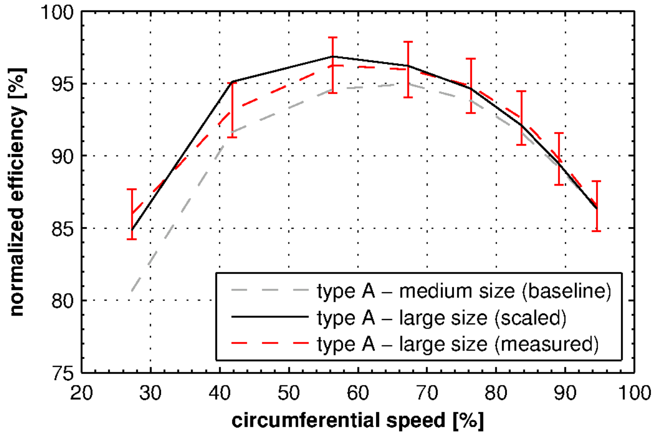

Figure 11 Comparison of the best-efficiency lines with a diameter scaling factor of 1.1

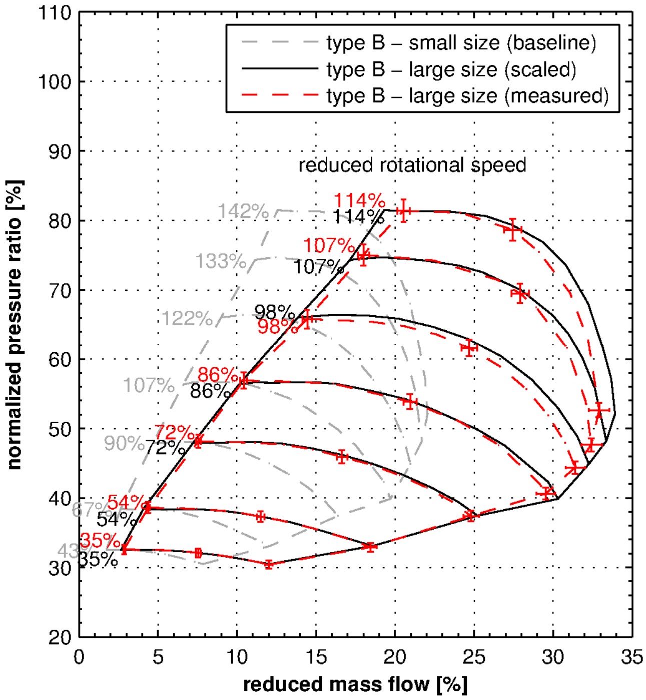

Figure 12 Map comparison with a diameter scaling factor of 1.24

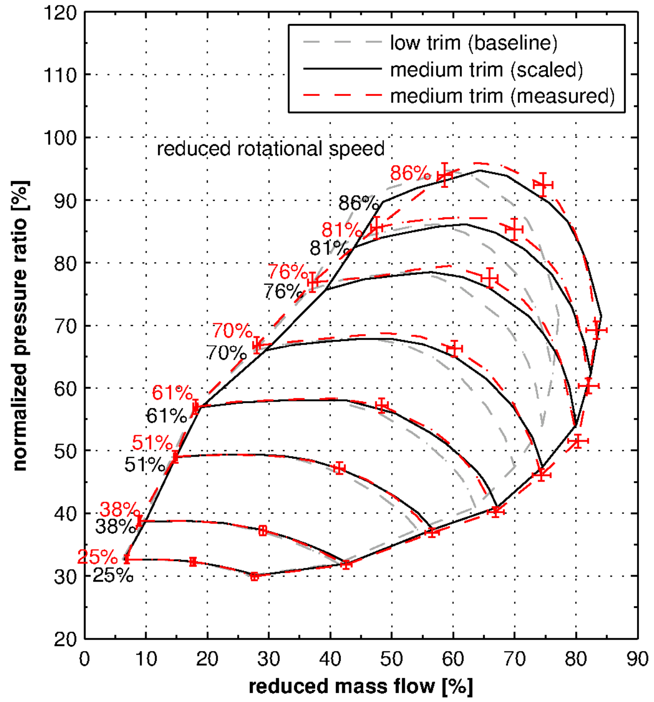

Figure 14 Map comparison with a trim scaling factor of 1.04

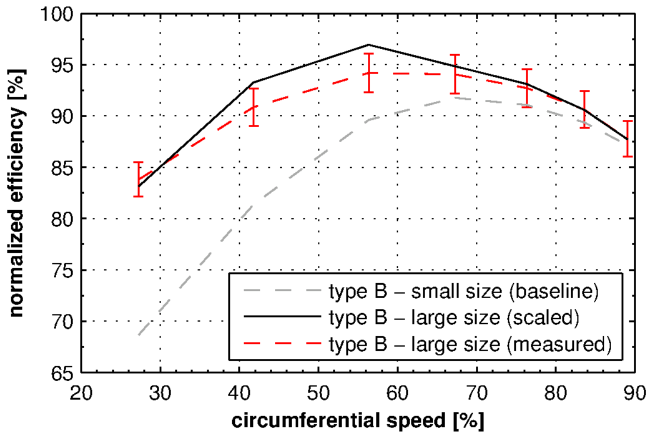

Figure 13 Comparison of the best-efficiency lines with a diameter scaling factor of 1.24

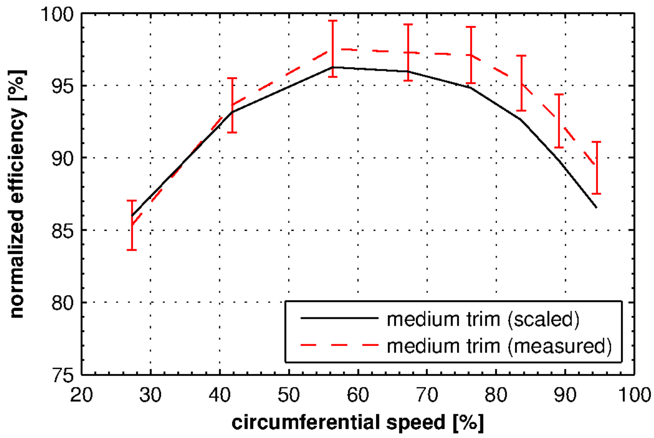

Figure 15 Comparison of the best-efficiency lines with a trim scaling factor of 1.04

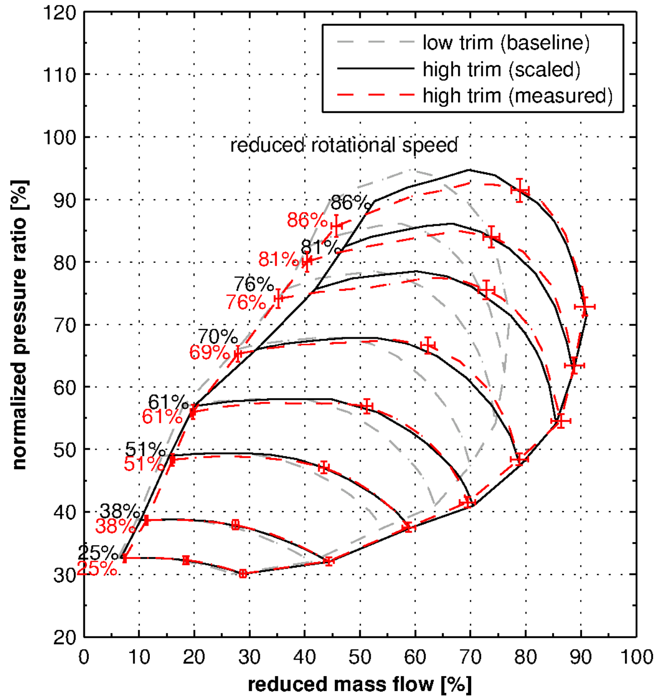

Figure 16 Map comparison with a trim scaling factor of 1.08

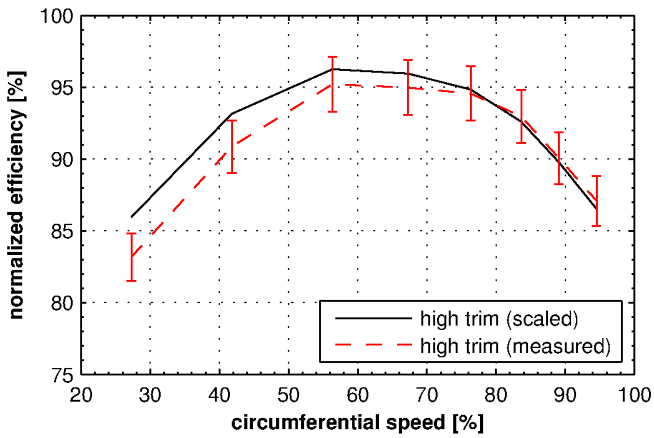

Figure 17 Comparison of the best-efficiency lines with a trim scaling factor of 1.08

REFERENCES

[1] Japikse, D., 1996. Centrifugal Compressor Design and Performance. Concepts ETI, Inc., Wilder, Vermont.

[2] Lakshminarayana, B., 1996. Fluid Dynamics and Heat Transfer of Turbomachinery. John Wiley & Sons, Inc., NYC.

[3] Whitfield, A., and Baines, N. C., 1990. Design of radial turbomachines. Longman, Harlow, Essex.

[4] Japikse, D., and Baines, N. C., 1994. Introduction to Turbomachinery. Concepts ETI, Inc., Norwich, Vermont.

[5] Baskharone, E. A., 2006. Principles of Turbomachinery in Air-Breathing Engines. Cambridge University Press, Cambridge.

[6] Shepherd, D. G., 1956. Principles of Turbomachinery. MacMillan Publishing Co., Inc., New York

[7] Schleer, M., and Abhari, R., 2005. "Influence of geometric scaling on the stability and range of a turbocharger centrifugal compressor". Proceedings of the ASME Turbo Expo 2005.

[8] Pampreen, R., 1973. "Small turbomachinery compressor and fan aerodynamics". J. of Engineering for Power, July 1973, pp. 251-256.

[9] Simon, H., and Buelskaemper, A., 1984. "On the Evaluation of Reynolds Number and Relative Surface Roughness Effects on Centrifugal Compressor Performance Based on Systematic Experimental Investigations". J. of Engineering for Gas Turbines and Power, 106, pp. 489-501.

[10] Casey, M. V., 1985. "The Effect of Reynolds Number on the Efficiency of Centrifugal Compressor Stages". J. of Engineering for Gas Turbines and Power, 107, pp. 541-548.

[11] Strub, R. A., Bonciani, L., Borer, C. J., Casey, M. V., Cole, S. L., Cook, B. B., Kotzur, J., Simon, H., and Strite, M. A., 1987. "Influence of the Reynolds Number on the Performance of Centrifugal Compressors". J. of Turbomachinery, 109(4), pp. 541-544.

[12] Rogers, C., 2001. "Centrifugal compressor blade trimming for a range of flows". Proceedings of ASME Turbo Expo 2001.

[13] Sapiro, L., 1983. "Effect of Extended Shrouds on Centrifugal Compressor Performance as a Function of Specific Speed". J. of Engineering for Power, 105(3), pp. 457-465.

[14] Engeda, A. 2007. "Effect of Impeller Exit Width Trimming on Compressor Performance". Proceedings of the 8th International Symposium on Experimental and Computational Aerodynamics of Internal Flows.

[15] Buckingham, E., 1914. "On physically similar systems: Illustration of the use of dimensional equations". Phys. Rev. 4(4).

[16] Dufour, G., Carbonneau, X., Cazalbou, J.-B., and Chassaing, P., 2006. "Practical use of similarity and scaling laws for centrifugal compressor design". Proceedings of the ASME Turbo Expo 2006 - Power for Land, Sea, and Air.

[17] Wright, T., 1989. "Comments on Compressor Efficiency Scaling with Reynolds Number and Relative Roughness". ASME Paper No. 89-GT-31.

ANNEX A

EFFICIENCY COMPARISONS

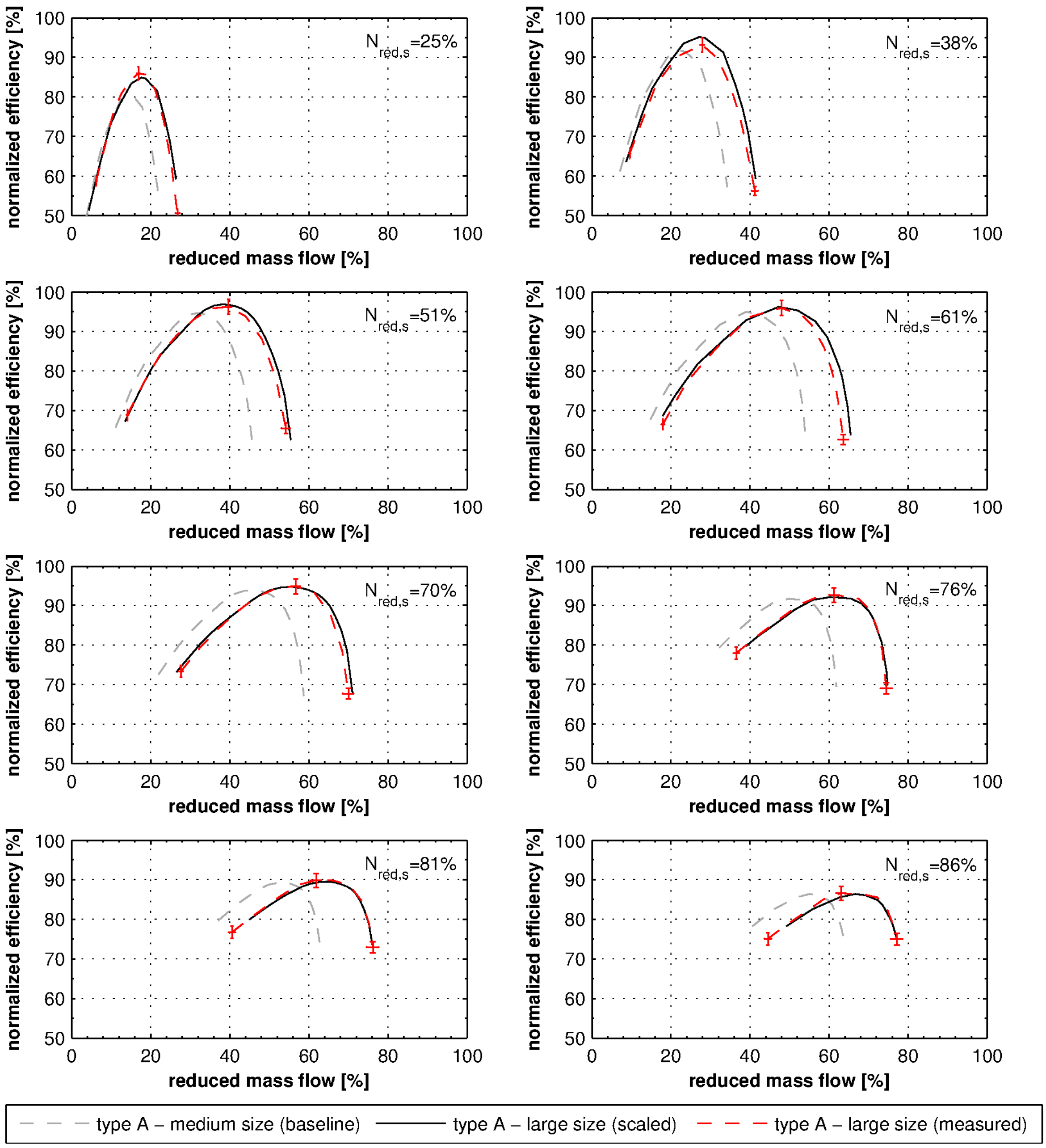

Figure 18 Comparison of the efficiency lines with a diameter scaling factor of 1.1

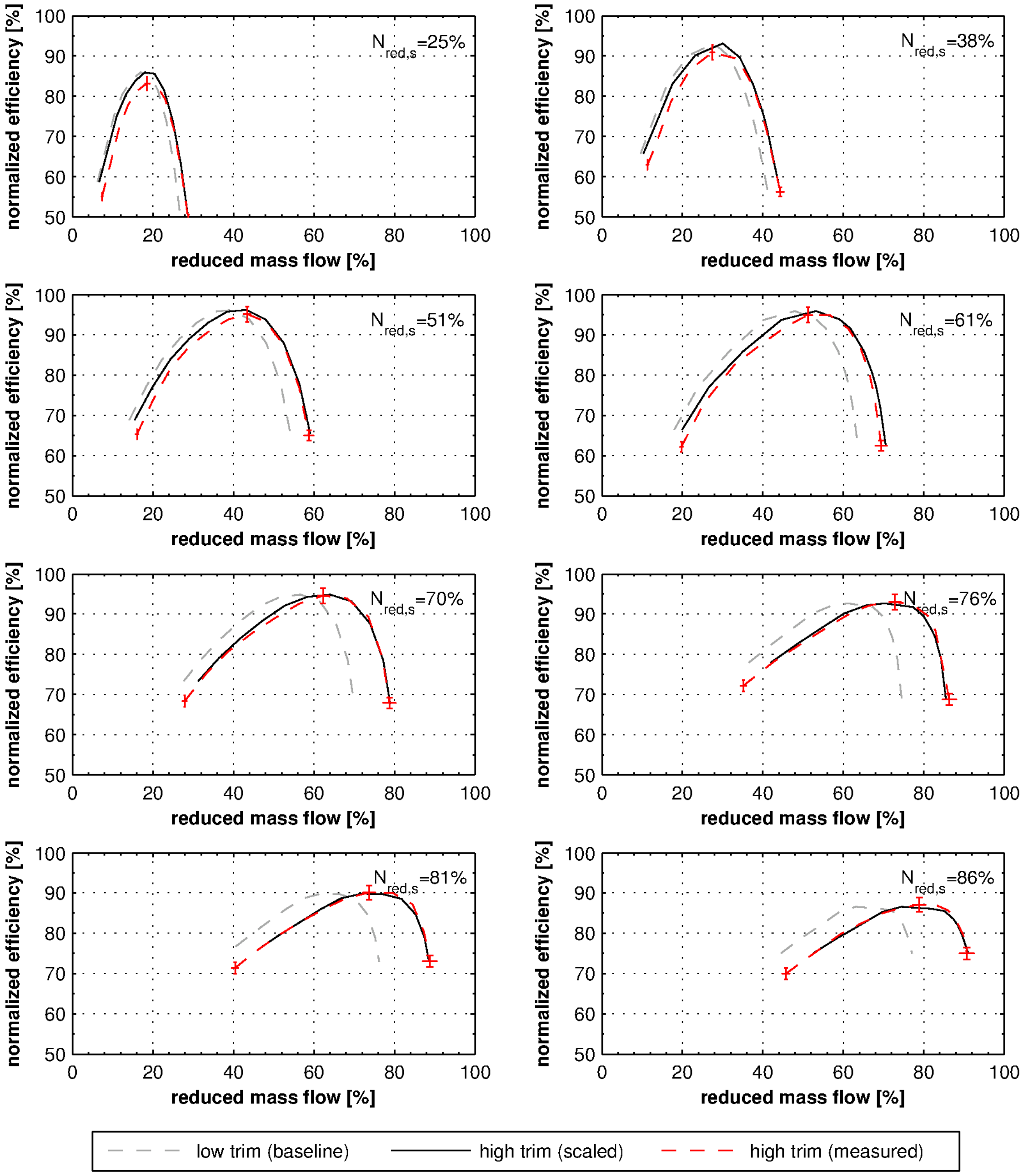

Figure 19 Comparison of efficiency lines with a trim scaling factor of 1.08